Desalination and Water Treatment
www.deswater.com

36 (2011) 141–151
December

1944-3994/1944-3986
doi: 10.5004/dwt.2011.2241

Utilization of agricultural waste chestnut shell for the removal of Reactive Brilliant Red K-2G from aqueous solution

Jing-Feng Gao*, Jin-Hui Wang, Quan Yuan, Chen Yang, Shu-Ying Wang, Yong-Zhen Peng

College of Environmental and Energy Engineering, Beijing University of Technology, 100 Pingleyuan, Chaoyang District, Beijing 100124, China.
Tel.: +861067391918; Fax: +861067392627; email: gao.jingfeng@bjut.edu.cn, gao158@gmail.com

Received 1 September 2010; accepted 11 May 2011

A B S T R A C T

Chestnut shell, an agricultural residue, was used as a low-cost adsorbent to remove Reactive Brilliant Red K-2G (RBR) from aqueous solution. Batch adsorption experiments were conducted to study the effects of initial solution pH value, adsorbent dosage, initial dye concentration and temperature on the adsorption. It was proved that strong acidic condition was favorable for the adsorption process and the optimal pH value was 1.0. Freundlich isotherm was appropriate for describing the experimental data. The kinetics study revealed that the adsorption of RBR onto chestnut shell followed the pseudo-second order model well. The external mass transfer mainly governed the adsorption rate. Thermodynamic studies demonstrated the spontaneous and exothermic natures of the adsorption process. The FTIR analysis indicated that functional groups such as amine, hydroxyl and phenolic compounds on the chestnut shell may be the active binding sites for the adsorption of RBR.

Keywords: Adsorption; Reactive Brilliant Red K-2G; Chestnut shell; Isotherm; Kinetic

1. Introduction

Synthetic dyes are widely used in the textile, plastic, paper, pulp, color photography, pharmaceutical and food industries. Most of the dyes are used in textile processing, in which its loss in wastewaters could vary from 2% for basic dyes to as high as 50% for reactive dyes, resulting in large amounts of dye-containing wastewater [1]. Furthermore, dye producers and users are interested in stability and fastness and are continually producing dyestuffs which are more difficult to degrade after use [2]. Thus, it is imperative to develop clean-up technologies for the treatment of water contaminated with dyes.

It is well known that activated carbons are the most largely adopted adsorbents for this process. However, the high unit cost of the activated carbon (about 1 US dollar/kg) and the absence of reliable methods for adsorbent regeneration (thermal regeneration costs are about 1–2 US dollar/kg) restrict its application [3]. So people have been searching for low-cost, renewable, locally available and efficient alternative adsorbents on and on. Based on the principle of waste control by waste, some researchers attempt to use agricultural waste materials to remove dyes from wastewater, including rice husk [4], sugarcane bagasse [5], wood apple shell [6] and wheat shell [7].

*Corresponding author

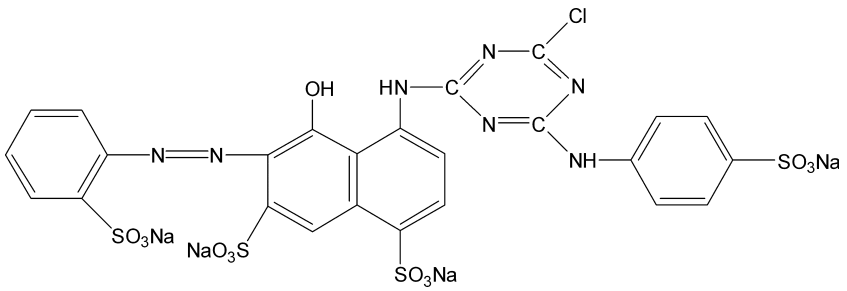

Fig. 1. Chemical structure of RBR.

In China, the production of chestnut is 9.25×10^5 tons in 2007, which is 75.61% of the total world production [8]. Chestnut shell is a residue of the food processing industry, it has no significant industrial and commercial values and will contribute to serious environmental problems without proper disposal [8]. In recent years, Ke et al. [9], Vázquez [10] and Yao et al. [8] have studied the application of chestnut shell on the heavy metals wastewater treatment. However, there are no reports on the use of chestnut shell as an adsorbent for dyes removal from aqueous solution.

Among dyes, water soluble reactive and acid dyes tend to pass through conventional treatment systems unaffected, hence, their removal is of great importance [11]. For the favorable characteristics of bright color and water-fast, Reactive Brilliant Red K-2G (RBR) was widely used in dyeing cotton and other cellulosic fibre. In this study, RBR was selected as a model compound.

Therefore, the main objective of this study was to examine the feasibility of using chestnut shell as an adsorbent to remove reactive dye from aqueous solution.

2. Materials and methods

2.1. Dye

RBR (C.I. Reactive Red 15, molecular formula = $C_{25}H_{14}ClN_7Na_4O_{13}S_4$, $\lambda_{max} = 512$ nm), was purchased from Tianjin Shengda Chemical Factory (China) and was used without further purification. Fig. 1 shows its molecular structure. All the working solutions used in the test were prepared by diluting the 200 mg/L of stock RBR solution to the desired concentrations. Prior to adding chestnut shell to the dye solution, the pH of each solution was adjusted to the required value with 0.1 mol/L HCl or NaOH solutions with a pH-meter (WTW 340i, Germany) for the measurements.

2.2. Preparation of the adsorbent

Prior to use, the chestnut shells were washed three times by deionized water to remove any adhering dirt, oven dried at 60°C for 48 h, crushed and sieved to obtain a particle size range of 0.6–1.0 mm.

2.3. Batch adsorption tests

Batch experiments were conducted in 50 mL Erlenmeyer flasks, which were agitated in a water bath shaker (GFL 1086, Germany) with a shaking rate of 150 rpm at a constant temperature until approaching equilibrium. Samples were taken at specified time intervals.

In order to investigate the effect of initial solution pH value on the adsorption capacity, the initial pH value varied in the range of 1–11, with the chestnut shell concentration fixed at 20 g/L and the initial RBR concentration of 50 mg/L. The optimal pH value (1.0 ± 0.1) was used for the subsequent experiments. To study the effect of adsorbent dosage, adsorbent concentration was varied from 8 to 40 g/L, initial RBR concentration was fixed at 50 mg/L and adsorbent dosage of 16 g/L was selected for the following experiments. In order to investigate the effect of initial dye concentration on adsorption, initial RBR concentration ranged from 30 to 150 mg/L. The equilibrium, kinetics and thermodynamic experiments were performed at temperatures in the range of 20–50°C and initial RBR concentration was in the range of 30–150 mg/L.

2.4. Analysis

The solution withdrawn from the flasks was clear enough to be analyzed after quick precipitation separation. The residual RBR concentration was determined by using a UV–vis spectrophotometer (UV-2802PC, Unico, Shanghai, China) at 512 nm.

The equilibrium adsorption capacity of RBR was calculated by using the following equation:

$$q_e = \frac{V(C_0 - C_e)}{m} \quad (1)$$

where C_0 and C_e are the initial and the equilibrium dye concentrations in the solution (mg/L); V is the volume

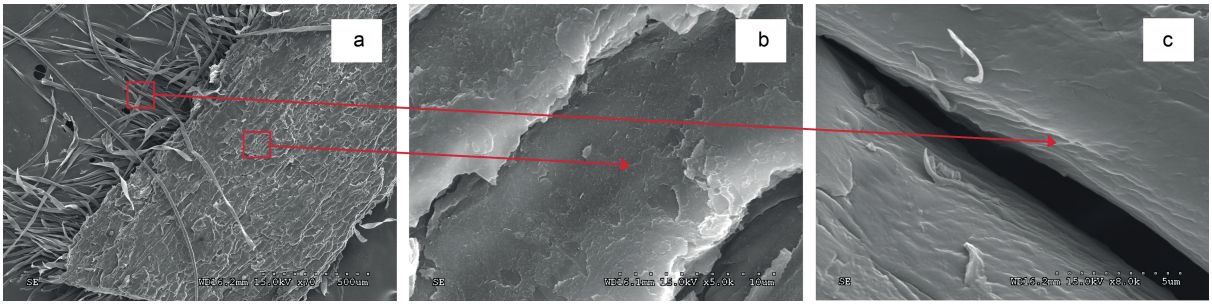

Fig. 2. SEM photographs of chestnut shell.

of the dye solution (L); and *m* is the weight of adsorbent used (g).

In order to characterize the surface functional groups presented on the adsorbent surface, the chestnut shells before and after adsorption were analyzed by Fourier Transform Infra-Red (FTIR) using a Bruker Vertex 70 FTIR spectrometer, which may reveal the possible dye binding mechanisms.

The textural properties of chestnut shell were measured by N_2 adsorption at 77 K in an ASAP 2020 apparatus (Micromeritics, USA).

3. Results and discussion

3.1. Characterization of the adsorbent

Fig. 2 shows the SEM photographs of chestnut shell. As seen from Fig. 2(a), the chestnut shell has heterogeneous surface and layered structure. Parts of chestnut was intact (Fig. 2(b)), also many tomentums were clearly found (Fig. 2(c)). The BET surface area, total pore volume and average pore diameter of the chestnut shell were found to be 0.474 m^2/g, 0.00064 cm^3/g and 5.39 nm, respectively. Its low BET surface area confirmed the presence of macropores. These properties increased the possibility of the dyes to be adsorbed onto chestnut shell.

Fig. 3 shows the FTIR spectra of the chestnut shell before and after RBR uptake in the range of 4000–400 cm^{-1}. The FTIR spectra before adsorption displayed a great number of absorption peaks, indicating the complex nature of the chestnut shell. The broad band at 3,298 cm^{-1} may be due to the overlapping of stretching vibration of O–H and N–H of hydroxyl and amine groups [11] on the surface of chestnut shell and the bands at 2,917 and 2,849 cm^{-1} might represent an asymmetric vibration of CH_2 [12] and stretching vibration of the C–H group. The band observed at 1,731 cm^{-1} could be due to a C=O group of a carboxylic acid or its ester. The bands at 1,594, 1,504 and 1,424 cm^{-1} could be attributed to the aromatic skeletal vibrations assigned to lignin or lignin-like material [13]. The band at

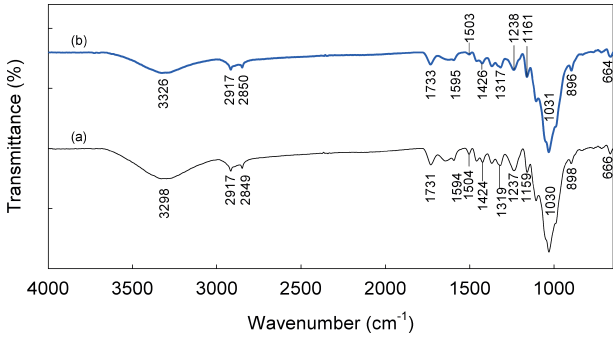

Fig. 3. FTIR spectra of chestnut shell before and after RBR adsorption. (a) before RBR adsorption and (b) after RBR adsorption.

1,319 cm^{-1} might represent the cellulose peak [14]. The presence of 1,237 cm^{-1} band was probably assigned to $-SO_3$ stretching [12]. The band at 1,159 cm^{-1} could be attributed to a combination of stretching vibration C–O–C of cellulose and stretching vibration of P=O [15]. The band at 1,030 cm^{-1} might indicate the presence of C–O group.

As shown in Fig. 3, there were significant similarities in the spectra before and after adsorption, suggesting that the components and structure of chestnut shell remained intact. After the RBR adsorption, the band intensity at 3,298 cm^{-1} decreased obviously and shifted to 3,326 cm^{-1}, one reason may be due to the N–H angular deformation [16], another reason may be the hydrogen bonds of O–H and N–H of hydroxyl and amine groups cleavage. The band intensity at 2,917 cm^{-1} decreased and did not shift, suggesting that some of the dyes molecules were adsorbed through a hydrophobic interaction between the CH_2 of chestnut shell and the hydrophobic part of the dye. The band at 2,849 cm^{-1} decreased and shifted to 2,850 cm^{-1}, indicating C–H group were involved in the adsorption. The band at 1,731 cm^{-1} shifted to 1,733 cm^{-1} and intensity decreased, indicating there would be an interaction between carboxylic acid or its ester and RBR. The band intensity at 1,594 and 1,424 cm^{-1} were clearly

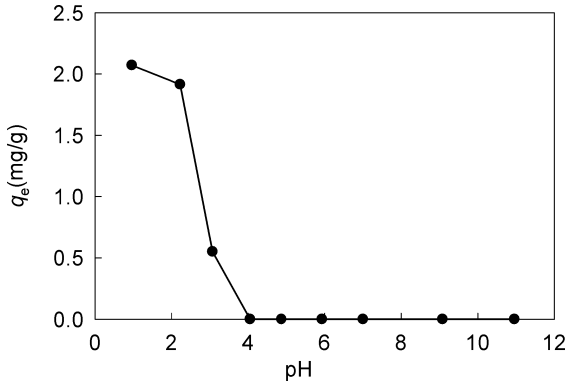

Fig. 4. Effects of initial pH value on RBR adsorption by chestnut shell (C_0 = 50 mg/L, adsorbent dosage = 20 g/L, temperature = 20 ± 1°C).

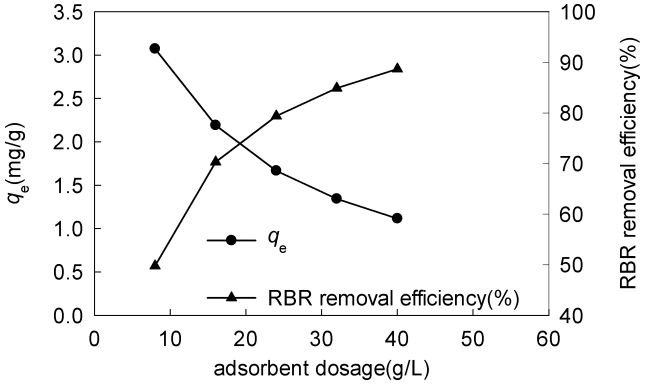

Fig. 5. Effect of adsorbent dosage on RBR adsorption by chestnut shell (C_0 = 50 mg/L, initial pH value = 1.0 ± 0.1, temperature = 20 ±1°C).

decreased, suggesting that aromatic compounds assigned to lignin or lignin-like material were involved in the adsorption. The band at 1,030 cm^{-1} decreased clearly and shifted to 1,031 cm^{-1}, indicating there would be an interaction between C–O group and RBR molecule. The FTIR analysis indicated that functional groups such as amine, hydroxyl and phenolic compounds on the chestnut shell may be the active binding sites for the adsorption of RBR.

3.2. The factors influencing RBR adsorption onto chestnut shell

3.2.1. Effect of initial solution pH value

As shown in Fig. 4, pH has a significant effect on the adsorption potential of RBR. The adsorption capacity decreased dramatically with the pH value increasing from 1.0 to 4.0 and adsorption process was restricted when the pH value was higher than 4.0. In this study, 90.8%, 72.9% and 21.7% dye removal were achieved at pH 1.0, 2.0 and 3.0, respectively, demonstrating that low pH value was favored. The maximum adsorption capacity was obtained at pH 1.0 and pH value of 1.0 was considered to be optimum.

It is well known that pH can affect the site dissociation of the biomass and the solution dye chemistry [17]. The point of zero charge (pH_{PZC}) of chestnut shell was 4.9 [8]. When the pH value was higher than pH_{PZC}, there was a net negative charge, which may result from the deprotonation of some functional groups on chestnut shell, such as carboxylate and phosphate groups. When the pH value was less than pH_{PZC}, protonation of the functional groups such as amino, resulted in a net positive charge. The interaction of the anionic ion (SO_3^-) produced by RBR with the amino groups ($R–NH_2$) on the chestnut shell may be one of the reasons for RBR adsorption [18], which is displayed in the following equations:

$$\underset{\text{chestnut shell}}{-NH_2} \overset{H^+}{\underset{\text{protonation}}{\rightleftharpoons}} -NH_3^+ \quad (2)$$

$$RBR-SO_3Na \overset{H_2O}{\underset{\text{dissociation}}{\rightleftharpoons}} RBR-SO_3^- + Na^+ \quad (3)$$

$$-NH_3^+ + RBR-SO_3^- \underset{\text{electrostatic interaction}}{\rightleftharpoons} -NH_3\cdots O_3S-RBR \quad (4)$$

The pH value of typical wastewater from a textile dyeing process ranges from 2 to 10 [19]. In most cases, the pH value of dyes wastewater is not optimal and needs proper adjustment. Waste acid addition may be one of the alternatives to adjust the pH of dyes wastewater.

3.2.2. Effect of adsorbent dosage

A plot of the adsorption capacity and RBR removal efficiency (%) vs. different chestnut shell concentration ranging from 8 to 40 g/L is shown in Fig. 5 and the initial RBR concentration was fixed at 50 mg/L. As expected the larger sorbent dosage the smaller dye concentration in solid phase and the larger dye removal efficiency. On the basis of this evidence, chestnut shell concentration of 16 g/L was selected as the optimal dosage and was used for the subsequent experiments.

3.2.3. Effect of initial dye concentration and contact time

Fig. 6 displays the amount of RBR adsorbed onto per unit mass of chestnut shell versus contact time at different initial dye concentrations ranging from 30 to 150 mg/L. As shown in Fig. 6, the uptake of RBR

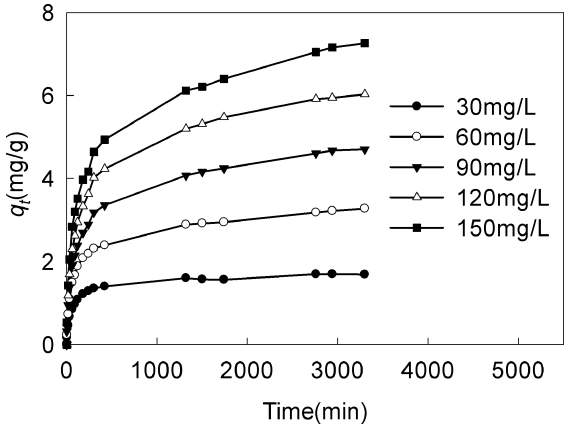

Fig. 6. Effect of initial dye concentration on RBR adsorption by chestnut shell (adsorbent dosage = 16 g/L, initial pH value = 1.0 ± 0.1, temperature = 20 ± 1°C).

increased with increasing contact time. Actually, a mass of RBR was removed in the initial 120 min for all of the initial concentrations studied with a gradual increase in the later stage. The time required for equilibrium was 22 h approximately, varying with the initial dye concentration slightly. In fact, long time contact in the later stage makes no significant contribution to the removal of RBR. In addition, the q_e increased from 1.69 to 7.26 mg/g with the initial dye concentration increasing from 30 to 150 mg/L.

3.3. Adsorption kinetics

In order to investigate the mechanisms of the adsorption process of RBR onto chestnut shell and to find out the rate-controlling steps, several kinetic models were used to analyze the experimental data, such as pseudo-first order kinetic model [20], pseudo-second order kinetic model [21], intraparticle diffusion kinetic model [22] and external mass transfer model [23].

The pseudo-first order equation is expressed as follows:

$$\log(q_e - q_t) = \log q_e - \frac{k_1 t}{2.303}. \quad (5)$$

Eq. (5) can be further rearranged into Eq. (6):

$$\frac{t}{q_t} = \frac{1}{k_1 q_e^2} + \frac{1}{q_e} t, \quad (6)$$

where q_t is the dye amounts adsorbed per unit mass of adsorbent at time t (mg/g) and k_1 is the pseudo-first order rate constant for the adsorption process (min^{-1}).

A plot of the linearized form of the pseudo-first order kinetic model is shown in Fig. 7(a). The values of k_1 and q_e are listed in Table 1. It has been reported that the pseudo-first order kinetic model exhibits a good fit to the experimental data well only in the initial adsorption period [21]. In the initial 30 min, the pseudo-first order kinetic model was used to describe the adsorption reluctantly with the correlation coefficients ranging from 0.9330 to 0.9729. However, it can not predict the adsorption capacity well, for all the calculated values of q_e were lower than those obtained from the experiments. So the adsorption of RBR onto chestnut shell does not follow pseudo-first order kinetics.

The pseudo-second order equation is written as follows:

$$\frac{t}{q_t} = \frac{1}{k_2 q_e^2} + \frac{1}{q_e} t, \quad (7)$$

where k_2 is the pseudo-second-order rate constant for the adsorption process (g/(mg min)).

Fig. 7(b) shows a plot of the linearized form of the pseudo-second-order kinetic model. The values of k_1 and theoretical q_e are all listed in Table 1 with the correlation coefficients. All the values of R^2 for the pseudo-second-order kinetic model were greater than 0.99 and the calculated values of q_e were almost equal to the experimental results. Furthermore, k_2 decreased with the increase of the initial dye concentrations. Hence, it is proved that the adsorption process of RBR onto chestnut shells can be satisfactorily described by a pseudo-second-order rate equation.

The adsorption of dye onto a solid phase material is a multi-step process and it is assumed to involve the following four steps: bulk diffusion, film diffusion, intraparticle diffusion and chemical reaction [17]. In the present study, the transportation of dye in the solution was very fast due to rapid shaking, so that the fist step cannot be rate limiting. And the fourth step is considered to be an equilibrium reaction, which is assumed to be rapid and negligible. So the experimental data were analyzed by using the intraparticle diffusion model [22] and external mass transfer model [23].

The intraparticle diffusion model can be expressed as follows:

$$q_t = k_{int} t^{1/2} + I, \quad (8)$$

where k_{int} is the intraparticle diffusion rate constant (mg/(mg·$min^{1/2}$)) and I is the intercept (mg/g), which is proportional to the thickness of the boundary layer.

As is shown in Fig. 7(c), the plot of q_t vs. $t^{1/2}$ was multilinear and there were two linear portions in general, which was indicative of two-stage diffusion of dyes onto chestnut shell. Similar results were reported for the adsorption of Basic Violet 3 and Acid Black 1

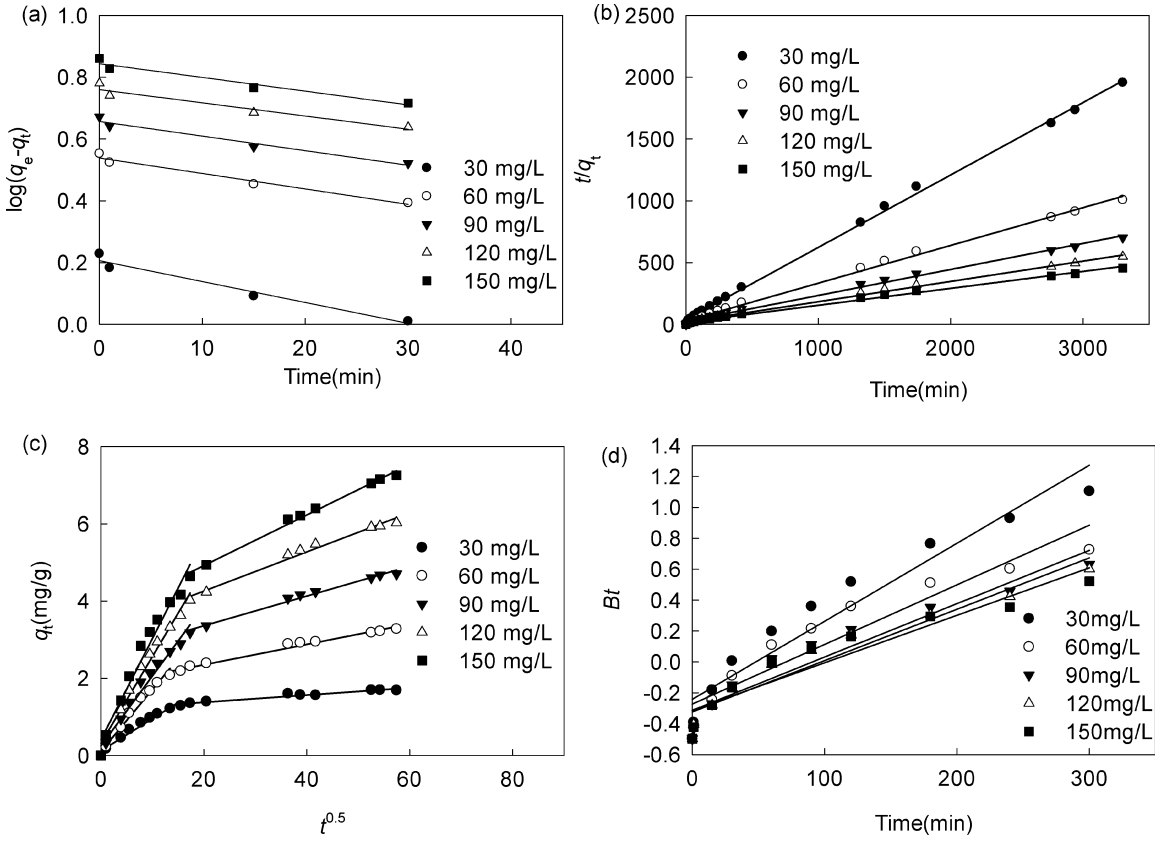

Fig. 7. Kinetic models for adsorption of RBR by chestnut shell at different initial concentrations (C_0 = 30, 60, 90, 120 and 150 mg/L, temperature = 20 ± 1 °C, adsorbent dosage = 16 g/L, initial pH value = 1.0 ± 0.1) (a) pseudo-first order model; (b) pseudo-second order model; (c) intraparticle diffusion model and (d) Boyd kinetics plot for RBR adsorption onto chestnut shell.

onto unburned carbon [24]. The initial section might represent the external mass transfer and the adsorption rate was relatively high. The second less steep section was probably attributed to the intraparticle diffusion. The values of k_{int} and I of the second linear portion are listed in Table 1. The values of the R^2 were high with a

Table 1
Rate constants of pseudo-first order, pseudo-second order and intraparticle diffusion kinetic models for the adsorption of RBR onto chestnut shell (temperature = 20 ± 1°C, adsorbent dosage = 16 g/L, initial pH value = 1.0 ± 0.1, C_0 = 30, 60, 90, 120 and 150 mg/L)

		C_0 (mg/L)				
Kinetic model	Parameter	30	60	90	120	150
Pseudo-first order	k_1 (min^{-1})	0.0157	0.0115	0.0108	0.0099	0.0103
	$q_{e,cal}$ (mg/g)	1.61	3.46	4.54	5.75	6.98
	R^2	0.9644	0.9729	0.9633	0.9330	0.9535
Pseudo-second order	k_2 (g/(mg·min))	0.0093	0.0034	0.0019	0.0014	0.0011
	$q_{e,cal}$ (mg/g)	1.71	3.27	4.75	6.09	7.29
	R^2	0.9987	0.9972	0.9964	0.9964	0.9947
Intraparticle diffusion	$q_{e,exp}$ (mg/g)	1.694	3.275	4.701	6.026	7.257
	k_{int}	0.0093	0.0264	0.0384	0.0507	0.0656
	I	0.0093	1.8220	2.5922	3.2413	3.6060
	R^2	0.9480	0.9803	0.9866	0.9832	0.9930

range of 0.9677−0.9815 for the initial section and 0.9480−0.9930 for the second section, expressing that both external mass transfer and intraparticle diffusion might be involved in the adsorption process. Further more, the intraparticle diffusion plots did not pass through the origin, indicating that intraparticle diffusion was not the only rate-controlling step.

In order to determine the actual rate-controlling step, the adsorption data were further analyzed by the kinetic expression proposed by Boyd et al. [23],

$$F = 1 - \frac{6}{\pi^2} e^{-Bt}, \tag{9}$$

where F is the fraction of solute adsorbed at different times t and Bt is a mathematical function of F and given by the following equation

$$F = \frac{q_t}{q_\alpha}, \tag{10}$$

where q_t and q_α represents the amount adsorbed (mg/g) at any time t and at infinite time (in the present study q_α was considered equal to q_e).

According to Eqs. (9) and (10), the kinetic expression can be rewritten as follows:

$$Bt = -0.4977 - \ln\left(1 - \frac{q_t}{q_\alpha}\right) \tag{11}$$

Thus the value of Bt can be calculated for each value of F according to Eq. (11). Fig. 7(d) shows that the relationship between calculated Bt values and time were linear but the lines did not pass through the origin, indicating that the external mass transfer mainly governed the rate-controlling process of RBR adsorption on chestnut shell. In addition, as the initial dye concentration decreased, the plot of Bt against time moved towards the origin, which indicates that intraparticle diffusion became rate controlling [25].

The controlling step occurred in the adsorption system depends on the specific system, such as the physico-chemical properties of the adsorbent and adsorbate. In order to maximize the efficiency of the adsorption system, the parameter selection should be made mainly on the basis of the controlling step.

3.4. Equilibrium isotherm

Isotherm models can be developed by analyzing the equilibrium data and the most appropriate model will be used to design the adsorption system in practice. In this work, four types of adsorption isotherm models were tested, including Langmuir [26], Freundlich [27], Temkin [28] and Dubinin–Radushkevich (D–R) isotherm [29]. Fig. 8 displays the q_e–C_e curves obtained at 20 ± 1, 35 ± 1 and 50 ± 1°C.

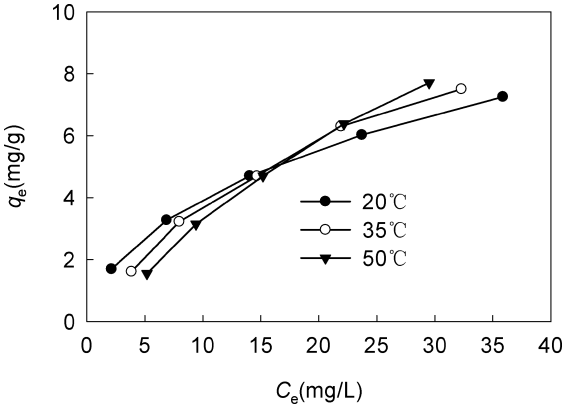

Fig. 8. q_e vs. C_e at different temperatures (adsorbent dosage = 16 g/L, initial pH value = 1.0 ± 0.1, temperature = 20 ± 1, 35 ± 1 and 50 ± 1°C).

The Langmuir equation is given as

$$q_e = \frac{q_m K_a C_e}{1 + K_a C_e}, \tag{12}$$

where q_m and K_a are Langmuir's constants related to the capacity (mg/g) and energy of the adsorption (L/mg), respectively.

The Langmuir equation can be written in the following linearized form:

$$\frac{1}{q_e} = \frac{1}{K_a q_m} \cdot \frac{1}{C_e} + \frac{1}{q_m}. \tag{13}$$

The linearized Langmuir adsorption isotherms are shown in Fig. 9. The values of K_a, q_m and the regression correlation coefficients are given in Table 2.

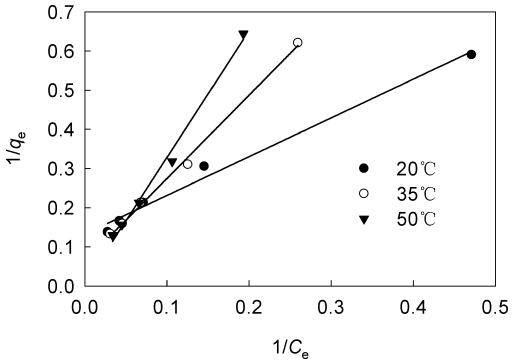

Fig. 9. Langmuir isotherms for RBR adsorption by chestnut shell at different temperatures. (C_0 = 30, 60, 90, 120 and 150 mg/L, adsorbent dosage = 16 g/L, initial pH value = 1.0 ± 0.1, temperature = 20 ± 1, 35 ± 1 and 50 ± 1°C).

Table 2
Isotherm parameters for the adsorption of RBR onto chestnut shell (adsorbent dosage = 16 g/L, initial pH value = 1.0 ± 0.1, C_0 = 30–150 mg/L, temperature = 20 ± 1, 35 ± 1 and 50 ± 1°C)

Isotherm	Parameter	Temperature (°C)		
		20	35	50
Langmuir	q_m (mg/g)	7.56	16.23	217.39
	K_a (L/mg)	0.1336	0.0289	0.0014
	R^2	0.9884	0.9971	0.9917
Freundlich	K_F (mg/g)(L/mg)$^{1/n}$	1.18	0.66	0.37
	N	1.94	1.38	1.09
	R^2	0.9979	0.9856	0.9880
Temkin	A (L/mg)	0.95	0.43	0.28
	B	1.94	2.78	3.53
	R^2	0.9732	0.9865	0.9853
D–R	Q_m (mmol/g)	6.20×10^{-6}	6.91×10^{-6}	7.48×10^{-6}
	$K_{DR}\times10^6$ (mol^2/kJ^2)	1400	4400	8200
	E (kJ/mol)	0.0267	0.0151	0.0110
	R^2	0.8178	0.8932	0.9191

Table 3
Reported q_m of some low-cost adsorbents for the adsorption of reactive dyes

Adsorbent	Dye	q_m (mg/g)	Reference
Activated sludge	Reactive Blue 2	250	[30]
Metal hydroxide sludge	Reactive Red 141	56.18	[31]
Waste metal hydroxide	Reactive Red 120	48.31	[32]
Modified palygorskite	Reactive Red 3BS	34.24	[33]
Fly ash	Reactive Black 5	7.94	[34]
Chestnut shell	RBR	7.56	This study
High lime fly ash	Reactive Black 5	7.18	[35]
Untreated alunite	Reactive Blue 114	2.92	[36]
	Reactive Red 124	2.85	
Anodonta shell	Reactive Green 12	0.436	[37]

According to Fig. 9 and Table 2, the correlation coefficients ranging from 0.9884 to 0.9971 and the value of K_a decreased with the increasing temperature, indicating that RBR molecules exhibited higher affinity for chestnut shell at lower temperature. However, q_m increased with the increasing temperature, which did not agree with the variation of K_a. So Langmuir isotherm was not appropriate for describing the RBR adsorption equilibrium on chestnut shell within the whole temperature range studied.

The maximum adsorption capacity (q_m) of other low-cost adsorbents for the adsorption of reactive dyes are listed in Table 3. In this study, the value of q_m was 7.56 mg/g, indicating chestnut shell was an alternative low-cost adsorbent for the treatment of RBR wastewater.

The Freundlich empirical equation is expressed by the following equation:

$$q_e = K_F C_e^{1/n}, \tag{14}$$

where K_F and n are the Freundlich constant ((mg/g)(L/mg)$^{1/n}$) and the heterogeneity factor, respectively. Eq. (14) could be transformed into the following linearized form:

$$\ln q_e = \ln K_F + \frac{1}{n}\ln C_e. \tag{15}$$

The Freundlich linear plots obtained at different temperatures are shown in Fig. 10. And the values of K_F, n and the regression correlation coefficients are all listed in Table 2. As shown in Fig. 10, the Freundlich model described the adsorption equilibrium well, with the correlation coefficients above 0.9880 at all the selected temperatures. The values of n were greater than unity, which suggests that the adsorption process of RBR onto chestnut shell was a favorable physical process. Both K_F and n decreased with the increasing temperature, indicating the exothermic nature of the adsorption. So Freundlich model can be used to describe the adsorption equilibrium of RBR onto chestnut shell successfully.

The general form of the Temkin isotherm is:

$$q_e = \frac{RT}{b}\ln AC_e. \tag{16}$$

Eq. (16) can be transformed into the following linear form:

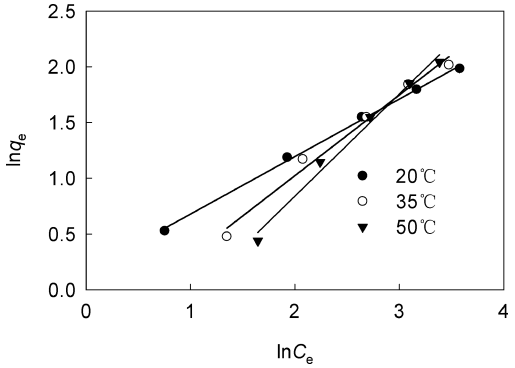

Fig. 10. Freundlich isotherms for RBR adsorption by chestnut shell at different temperatures. (C_0 = 30, 60, 90, 120 and 150 mg/L, adsorbent dosage = 16 g/L, initial pH value = 1.0 ± 0.1, temperature = 20 ± 1, 35 ± 1 and 50 ± 1°C).

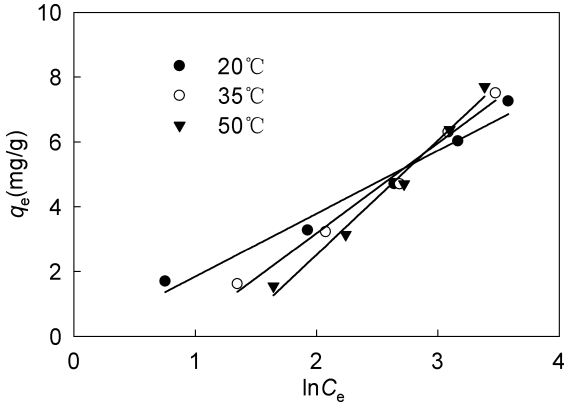

Fig. 11. Temkin isotherms for RBR adsorption by chestnut shell at different temperatures. (C_0 = 30, 60, 90, 120 and 150 mg/L, adsorbent dosage = 16 g/L, initial pH value = 1.0 ± 0.1, temperature = 20 ± 1, 35 ± 1 and 50 ± 1 °C).

$$q_e = B \ln A + B \ln C_e, \tag{17}$$

where R is the gas constant (8.314 J/(mol·K)); T is the absolute temperature (K); A is the equilibrium binding constant (L/mg); B is the Temkin isotherm constant related to the heat of adsorption and $B = RT/b$.

Fig. 11 shows the Temkin linear plots. The values of A and B are given in Table 2 along with the correlation coefficients. The B value increased with the temperature increasing from 20 to 50°C, which disagreed with the variation of A, indicating that Temkin isotherm could not be used to describe the studied adsorption process.

The D–R equation has been applied in the following form:

$$q_e = Q_m e^{-K_{DR}\varepsilon^2}. \tag{18}$$

A linear form of the D–R isotherm is:

$$\ln q_e = \ln Q_m - K_{DR}\varepsilon^2, \tag{19}$$

where Q_m represents the theoretical saturation adsorption capacity (mmol/g), K_{DR} is a constant related to the adsorption energy (mol^2/kJ^2) and ε is the Polanyi potential which is determined by the following equation:

$$\varepsilon = RT \ln\left(1 + \frac{1}{C_e}\right), \tag{20}$$

where R is the gas constant and T is the absolute temperature.

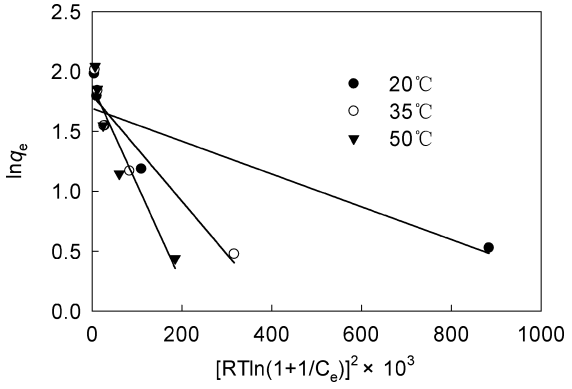

Fig. 12. D–R isotherms for RBR adsorption by chestnut shell at different temperatures. (C_0 = 30, 60, 90, 120 and 150 mg/L, adsorbent dosage = 16 g/L, initial pH value = 1.0 ± 0.1, temperature = 20 ± 1, 35 ± 1 and 50 ± 1 °C).

The mean free energy of adsorption (E) could be calculated from the K_{DR} value using the following relation:

$$E = \frac{1}{\sqrt{2K_{DR}}}. \tag{21}$$

Fig. 12 shows the D–R isotherm plots and the values of Q_m, K_{DR}, E and R^2 are all given in Table 2. In this study, the E values were 0.027, 0.015 and 0.011 kJ/mol at 20, 35 and 50°C, respectively, which was much lower than 8 kJ/mol, suggesting that the adsorption process of both dyes might be physical in nature [38]. E decreased with the increasing temperature, however, Q_m of 35 and 50°C were all higher than that of 20°C, indicating D–R model was not fit for the experimental data.

3.5. Thermodynamic analysis

The thermodynamic parameters commonly used include Gibbs free energy change (ΔG°), enthalpy change (ΔH°) and entropy change (ΔS°), which can reflect the adsorption characteristics of an adsorbent and are key factors to be considered in the adsorption system design. Moreover, the possible mechanisms of adsorption can be understood by evaluation of the thermodynamic parameters [17].

The thermodynamic parameters are calculated according to Eq. (22) and Van't Hoff (Eq. (23))

$$\Delta G^o = -RT \ln K_p, \tag{22}$$

$$\ln K_p = \frac{\Delta S^o}{R} - \frac{\Delta H^o}{RT}, \tag{23}$$

where R is the gas constant, T is temperature in K and K_p is the thermodynamic equilibrium constant (the

Table 4
Thermodynamic parameters of RBR adsorption by chestnut shell

T (K)	ΔG° (kJ/mol)	ΔH° (kJ/mol)	ΔS° (J/(mol·K))
293	−4.30	−5.42	−3.85
305	−4.01		
323	−3.80		

ratio of the equilibrium concentration of chestnut shell on the adsorbent to that in the solution, $K_p = (C_0 - C_e)/C_e$, C_0 = 30, 60, 90, 120 and 150 mg/L). The values of ΔG° at different temperatures are listed in Table 4. The values of ΔH° and ΔS° obtained from the slope and intercept of the plot of $\ln K_p$ vs. $1/T$ (Figure are not shown here, $R^2 = 0.9966$) are also summarized in Table 4. At constant temperature and pressure, the ΔG° value is the fundamental criterion of spontaneity [17] and the negative values of ΔG° for the adsorption at all temperatures indicate that the adsorption of RBR onto chestnut shell is spontaneous in nature. Typically, the range of ΔH° for physical adsorption and chemical adsorption are −4 to −40 kJ/mol and −40 to −800 kJ/mol [17], respectively. For this study, the ΔH° value was −5.42 kJ/mol, the adsorption process might be considered as physical adsorption and the negative ΔH° value also suggests the exothermic nature of the adsorption. As for ΔS°, the negative value of −3.85 J/(mol·K) indicates a decrease in freedom degree of the adsorption systems.

4. Conclusions

Chestnut shell, an agricultural waste and easily available material, was investigated as an adsorbent to remove RBR from aqueous solutions. The experimental results revealed that the adsorption of RBR onto chestnut shell was highly dependent on the acidic pH and the optimal pH value was 1.0. Freundlich isotherm fitted well with the experimental data. Kinetic analysis indicates that the adsorption of RBR onto chestnut shell followed the pseudo-second order model and both the external mass transfer and the intraparticle diffusion were observed in the adsorption, with the former step being the rate-controlling process. According to the thermodynamic analysis, this adsorption process was spontaneous and exothermic in nature. FTIR analysis shows that the adsorption of RBR may be attributed to functional groups such as amine, hydroxyl and phenolic compounds on the chestnut shell. Based on the results of this study, chestnut shell could be used as a low-cost efficient and alternative adsorbent for the removal of RBR from wastewater. It is expected that the information provided here would be useful for further research on these critical issues and its application for the treatment of dyes wastewater.

Acknowledgements

The authors wish to thank the National Natural Science Foundation of China (51078007), National University Student Innovative Experiment Project (101000514), Natural Science Foundation of Beijing (8112007) and Funding Project for Academic Human Resources Development in Institutions of Higher Learning under the Jurisdiction of Beijing Municipality (PHR20110819) for the financial supports of this study.

References

[1] H. Ali, Biodegradation of synthetic dyes-A review, Water, Air, Soil Pollut., 213 (2010) 251–273.
[2] E.Y. Ozmen, S. Erdemir, M. Yilmaz and M. Bahadir, Removal of carcinogenic direct azo dyes from aqueous solutions using calix[n]arene derivatives, CLEAN – Soil, Air, Water, 35 (2007) 612–616.
[3] M.E. Russo, F. Di Natale, V. Prigione, V. Tigini, A. Marzocchella and G.C. Varese, Adsorption of acid dyes on fungal biomass: Equilibrium and kinetics characterization, Chem. Eng. J., 162 (2010) 537–545.
[4] W. Zou, P. Han, Y. Li, X. Liu, X. He and R. Han, Equilibrium, kinetic and mechanism study for the adsorption of neutral red onto rice husk, Desalin. Water Treat., 12 (2009) 210–218.
[5] S. A. Saad, K.M. Isa and R. Bahari, Chemically modified sugarcane bagasse as a potentially low-cost biosorbent for dye removal, Desalination, 264 (2010) 123–128.
[6] S. Jain and R.V. Jayaram, Removal of basic dyes from aqueous solution by low-cost adsorbent: Wood apple shell (*Feronia acidissima*), Desalination, 250 (2010) 921–927.
[7] Y. Bulut and H. AydIn, A kinetics and thermodynamics study of methylene blue adsorption on wheat shells, Desalination, 194 (2006) 259–267.
[8] Z.Y. Yao, J.H. Qi and L.H. Wang, Equilibrium, kinetic and thermodynamic studies on the biosorption of Cu(II) onto chestnut shell, J. Hazard. Mater., 174 (2010) 137–143.
[9] X. Ke, P. Li, Q. Zhou, Y. Zhang and T. Sun, Removal of heavy metals from a contaminated soil using tartaric acid, J. Environ. Sci., 18 (2006) 727–733.
[10] G. Vazquez, M. Calvo, M. Sonia Freire, J. Gonzalez-Alvarez and G. Antorrena, Chestnut shell as heavy metal adsorbent: Optimization study of lead, copper and zinc cations removal, J. Hazard. Mater., 172 (2009) 1402–1414.
[11] J.F. Gao, Q. Zhang, K. Su and J.H. Wang, Competitive biosorption of Yellow 2G and Reactive Brilliant Red K-2G onto inactive aerobic granules: Simultaneous determination of two dyes by first-order derivative spectrophotometry and isotherm studies, Bioresour. Technol., 101 (2010) 5793–5801.
[12] G. Vázquez, M. Sonia Freire, J. González-Alvarez and G. Antorrena, Equilibrium and kinetic modelling of the adsorption of Cd^{2+} ions onto chestnut shell, Desalination, 249 (2009) 855–860.
[13] J.G. Buta and G.C. Galletti, FT-IR investigation of lignin components in various agricultural lignocellulosic by-prod, J. Sci. Food Agric., 49 (1989) 37–43.
[14] N.M. Morris, E.A. Catalano and B.A.K. Andrews, FT-IR Determination of degree of esterification in polycarboxylic acid cross-link finishing of cotton, Cellulose, 2 (1995) 31–39.

[15] J. Mao, S.W. Won and Y.S. Yun, Biosorption of reactive and basic dyes using fermentation waste Corynebacterium glutamicum: The effects of pH and salt concentration and characterization of the binding sites, World J. Microbiol. Biotechnol., 25 (2009) 1259–1266.
[16] A.C. Lucilha, C.E. Bonancea, W.J. Barreto and K. Takashima, Adsorption of the diazo dye Direct Red 23 onto a zinc oxide surface: A spectroscopic study, Spectrochim. Acta, Part A, 75 (2010) 389–393.
[17] G. Crini and P.M. Badot, Application of chitosan, a natural aminopolysaccharide, for dye removal from aqueous solutions by adsorption processes using batch studies: A review of recent literature, Prog. Polym. Sci., 33 (2008) 399–447.
[18] J. Gao, Q. Zhang, K. Su, R. Chen and Y. Peng, Biosorption of Acid Yellow 17 from aqueous solution by non-living aerobic granular sludge, J. Hazard. Mater., 174 (2010) 215–225.
[19] W. Lau and A.F. Ismail, Polymeric nanofiltration membranes for textile dye wastewater treatment: Preparation, performance evaluation, transport modelling, and fouling control – a review, Desalination, 245 (2009) 321–348.
[20] S. Lagergren, Zur theorie der sogenannten adsorption gelöster stoffe, K. Sven. Vetenskapsakad. Handl., 24 (1898) 1–39.
[21] Y.S. Ho and G. McKay, Pseudo-second order model for sorption processes, Process. Biochem., 34 (1999) 451–465.
[22] W.J. Weber and J.C. Morris, Kinetics of adsorption on carbon from solution, J. Sanit. Eng. Div., ASCE, 89 (1963) 31–59.
[23] G.E. Boyd, A.W. Adamson and L.S. Myers, The exchange adsorption of ions from aqueous solutions by organic zeolites. II. Kinetics, J. Am. Chem. Soc., 69 (1947) 2836–2848.
[24] S. Wang and H. Li, Kinetic modelling and mechanism of dye adsorption on unburned carbon, Dyes Pig., 72 (2007) 308–314.
[25] A.E. Ofomaja, Kinetics and mechanism of methylene blue sorption onto palm kernel fibre, Process Biochem., 42 (2007) 16–24.
[26] I. Langmuir, The adsorption of gases on plane surfaces of glass, mica and platinum, J. Am. Chem. Soc., 40 (1918) 1361–1403.
[27] H. Freundlich, Ueber die adsorption in loesungen, Z. Phys. Chem., 57 (1907) 385–470.
[28] M. Temkin and V. Pyzhev, Recent modification to Langmiur isotherms, Acta Physiochim. USSR, 12 (1940) 217–222.
[29] M.M. Dubinin, E.D. Zaverina and L.V. Radushkevich. Sorption and structure of active carbons. I. Adsorption of organic vapors, J. Phys. Chem. [URSS], 21 (1947) 1351–1362.
[30] Z. Aksu, Biosorption of reactive dyes by dried activated sludge: equilibrium and kinetic modelling, Biochem. Eng. J., 7 (2001) 79–84.
[31] S. Netpradit, P. Thiravetyan and, S. Towprayoon, Application of 'waste' metal hydroxide sludge for adsorption of azo reactive dyes, Water Res., 37 (2003) 763–772.
[32] S. Netpradit, P. Thiravetyan and S. Towprayoon, Evaluation of metal hydroxide sludge for reactive dye adsorption in a fixed-bed column system, Water Res., 38 (2004) 71–78.
[33] A. Xue, S. Zhou, Y. Zhao, X. Lu and P. Han, Adsorption of reactive dyes from aqueous solution by silylated palygorskite, Appl. Clay Sci., 48 (2010) 638–640.
[34] Z. Eren and F.N. Acar, Adsorption of Reactive Black 5 from an aqueous solution: equilibrium and kinetic studies, Desalination, 194 (2006) 1–10.
[35] Z. Eren and F.N. Acar, Equilibrium and kinetic mechanism for Reactive Black 5 sorption onto high lime Soma fly ash, J. Hazard. Mater., 143 (2007) 226–232.
[36] M. Özacar and I.A. Sengil, Adsorption of reactive dyes on calcined alunite from aqueous solutions, J. Hazard. Mater., 98 (2003) 211–224.
[37] S.A. Figueiredo, R.A. Boaventura and J.M. Loureiro, Color removal with natural adsorbents: Modeling, simulation and experimental, Sep. Purif. Technol., 20 (2000) 129–141.
[38] F. Helfferich, Ion Exchange. McGraw-Hill, New York, USA, 1962.